

RSC Advances



This is an *Accepted Manuscript*, which has been through the Royal Society of Chemistry peer review process and has been accepted for publication.

Accepted Manuscripts are published online shortly after acceptance, before technical editing, formatting and proof reading. Using this free service, authors can make their results available to the community, in citable form, before we publish the edited article. This *Accepted Manuscript* will be replaced by the edited, formatted and paginated article as soon as this is available.

You can find more information about *Accepted Manuscripts* in the [Information for Authors](#).

Please note that technical editing may introduce minor changes to the text and/or graphics, which may alter content. The journal's standard [Terms & Conditions](#) and the [Ethical guidelines](#) still apply. In no event shall the Royal Society of Chemistry be held responsible for any errors or omissions in this *Accepted Manuscript* or any consequences arising from the use of any information it contains.

Ultrafast chemical lithiation of single crystalline silicon nanowires: in-situ characterization and first principles modeling

Jong-Hyun Seo^{a,b,1}, Chia-Yun Chou^{c,1}, Yu-Hao Tsai^c, Yigil Cho^d, Tae-Yeon Seong^b, Woo-Jung Lee^e, Mann-Ho Cho^e, Jae-Pyoung Ahn^a, Gyeong S. Hwang^{c,f,*} and In-Suk Choi^{d,*}

^a*Advanced Analysis Center, Korea Institute of Science and Technology, Seoul 130-650, South Korea*

^b*Department of Materials Science and Engineering, Korea University, Seoul 136-701, South Korea*

^c*Materials Science and Engineering Program, University of Texas at Austin, Austin, Texas 78712, United States*

^d*High Temperature Energy Materials Research Center, Korea Institute of Science and Technology, Seoul 130-650, South Korea*

^e*Institute of Physics and Applied Physics, Yonsei University, Seoul 120-749, Korea*

^f*Department of Chemical Engineering, University of Texas at Austin, Austin, TX 78712, United States*

* Corresponding Authors. Tel.: +82 2 958 6622; fax: +82 2 958 5449 (I.S. Choi) Tel: +1 512 471 4847; fax: +1 512 471 0542 (G.S. Hwang)
E-mail addresses: insukchoi@kist.re.kr (I.S. Choi) and gshwang@che.utexas.edu (G.S. Hwang)

¹ These authors are contributed equally to this work.

Keywords: Lithium ion battery, silicon nanowire, lithiation kinetics, density functional theory, in-situ test

Abstract

Through a combined density functional theory and in-situ scanning electron microscopy study, we provide the evidence of the ultrafast chemical lithiation of a single crystalline Si nanowire which is brought to direct contact with Li metal in the absence of an applied external electric field. Unlike the previous in-situ lithiation results, the ultra-fast lithiation process in this study is purely driven by the concentration gradient and is found to be limited by Li diffusion through the pristine/lithiated Si phase boundary. The experimental and calculated lithiation

speeds are in excellent agreement around 1 $\mu\text{m/s}$, corresponding to the high Li diffusivity value of about $10^{-9} \text{ cm}^2/\text{s}$. The improved understanding of lithiation kinetics may contribute to the design of higher-power Si-based anodes.

Introduction

Silicon (Si) has recently emerged as an attractive anode material for lithium-ion batteries (LIBs) because of its impressive energy storage capacity. Among all the potential anode materials, Si has the highest known theoretical capacity,¹⁻⁴ which is one order of magnitude larger than that of graphite (the most commonly used anode in today's Li-ion batteries).⁴⁻⁶ However, alloying Li with Si is a different process from Li insertion in graphite (via intercalation mechanism). The alloying-induced structural and volume changes (>300%) can cause pulverization, loss of electrical contact and consequently early capacity fading.^{2-4, 7-9} In order to overcome this drawback, many studies have approached the cyclability issue via structural modifications in the nanosize range.^{1, 10-14} It has been shown that because of the high surface-to-volume ratio, nanostructured Si can better accommodate strain and limit crack propagation, while the shorter diffusion distances for Li atoms offer the additional advantage of faster charging/discharging rates.^{1, 15-17} In recent years, a number of published works on Si have realized stable charge-discharge capacities over 1200 mAh/g for more than 1000 cycles,¹⁸ suggesting a great potential for application in LIBs.

Benefited by the development of in-situ test methods in electron microscopy (EM) and rapid advancement of atomistic scale modeling, significant progress has been made in the understanding of lithiation-induced structural evolution in nanostructured Si-based anodes.¹⁹⁻²¹ However, an affirmative description of Li kinetics in Si nanostructures is still very limited, and the experimentally measured Li diffusivity (D_{Li}) values are measured via electrochemical testing which vary by six orders of magnitude depending on the sample and test conditions.^{19, 22-24} Furthermore, since the conventional electrochemical approaches to D_{Li} determination are

based on an averaged property from ex-situ measurements, it is very difficult to characterize Li diffusion inside an individual nanowire and differentiate which from diffusion in electrolyte, through the complex solid-electrode-interface (SEI), and inside lithiated Si with varying Li concentrations.

In this paper, we present a combined experimental and theoretical investigation on the chemical lithiation of individual Si nanowires (NWs), which are brought to direct contact with Li metal inside a scanning microscope (SEM) in the absence of an applied electric field. Upon lithiation, the structural evolution is monitored in-situ, allowing us to estimate the propagation speed of the lithiation front which is faster than that of the previously reported ultra-fast lithiation of SiNWs,²² and correlate which with D_{Li} across the phase boundary between the lithiated and pristine Si. Together with the DFT investigations, we are able to explain the lithiation mechanism and more importantly reveal the genuine features of Li transport in lithiated SiNWs for the first time.

Experimental

Fabrication of single crystalline Si nanowires

Si NWs with [111] axial orientation were synthesized on the Si (111) substrate with Au catalyst by the vapor–liquid–solid (VLS) method using an ultrahigh vacuum chemical vapor deposition (CVD) system. A 2 nm thick Au film (as a catalyst) was deposited on a cleaned Si (111) substrate in a metal growth chamber at a growth pressure of $\sim 5 \times 10^{-7}$ Torr by thermal evaporation. After the formation of Au droplets through annealing, Si NWs were synthesized by filling the main chamber with a mixture of SiH₄ as precursors, and H₂ as the carrier gas, while maintaining a fixed total pressure of 2 Torr. The process temperature was set to 400–450°C at Au-Si eutectic temperatures. The dimension of grown Si NWs is approximately 2–3

μm in length and 70-110 nm in diameter as shown in Fig. S1. The more detailed information of synthesis and the structure of NWs are provided in the supporting information

In-situ direct contact lithiation

The direct solid state lithiation test without an external electrical potential was performed using a nanomanipulator (MM3A, Kleindiek). To avoid oxidation, the entire process was carried out inside the dual beam focused ion beam chamber (FIB, Quanta 3D, FEI). We transferred a Si nanowire from the substrate to the nanomanipulator tungsten tip by Pt deposition in the FIB chamber. The bulk Li was cut inside the chamber to make a pristine surface. Subsequently, we translated the harvested Si NW to the bulk Li and made direct contact of the fractured side end of the Si NW to the surface of the bulk Li. Please see the Fig. S2 for the schematic of the method in the supporting information. The whole process of the lithiation was exposed to the electron beam in SEM. therefore it may be possible to accumulate charges at different materials. However the tungsten probe and stage link to ground so electron beam haven't an effect on lithiation behavior. Moreover we conformed that the lithiation behavior occurs at turn off the electron beam.

Computational methods

Quantum mechanical calculations reported herein were performed on the basis of density functional theory (DFT) within the generalized gradient approximation (GGA-PW91), as implemented in the Vienna Ab-initio Simulation Package (VASP). The projected augmented wave (PAW) method with a plane-wave basis set was used to describe the interaction between core and valence electrons. An energy cutoff of 350 eV was used for geometric optimization of model structures for (i) $a\text{-LiSi}$ and $a\text{-Li}_2\text{Si}$, and (ii) $a\text{-Li}_4\text{Si/Si}(110)$ interface [Fig. 4]; all atoms were fully relaxed using the conjugate gradient method till residual forces are smaller than 5×10^{-2} eV/Å. For Brillouin zone sampling, sufficient k -point mesh was used in the

scheme of Monkhorst-Pack. To simulate the diffusion and chemical lithiation processes, ab initio molecular dynamics (AIMD) simulations were performed at the temperatures of interest; a time step of 1 fs was used while the temperature was controlled via Nose-Hoover thermostat. For more detailed simulation methods, please refer to the supporting information.

Results and discussions

In-situ characterization of chemical lithiation

Fig. 1 shows the microstructural evolution of an pristine Si [111] nanowire (SiNW), which was brought into direct contact with Li metal at room temperature in vacuum, without an external electric field (see Supporting information, Fig. S1, Fig. S2 and Movie 1 for detailed experimental methods and real-time in-situ lithiation behavior). At $t = 0.00$ s, the pristine SiNW was straight with a uniform diameter around 78.9 nm. Once the nanowire contacted bulk Li, it exhibited significant morphological changes captured in the time-lapse series of SEM images up to $t = 1.02$ s. Li atoms near the vicinity of the Li-Si contacting area diffused into the Si nanowire, and volume expansion occurred instantaneously as the effective reaction front (marked by the yellow triangle) propagated rapidly from the nanowire tip towards the other end. At $t = 1.02$, the entire SiNW swelled uniformly in the radial direction without noticeable elongation or bending.

The cross-section becomes circular after lithiation and the total volume expansion is estimated around 330 % which is comparable to that of a highly lithiated Si alloy (see Supporting information, Fig. S3 and Fig. S5).¹⁶ The scanning transmission electron microscope (STEM) and electron energy loss spectroscopy (EELS) analyses later confirmed the complete amorphization in the center of the lithiated SiNW (see Supporting information, Fig. S4). Different from the conventional electrochemical lithiation, our results clearly demonstrate that lithiation of a SiNW can occur in the absence of an external electric field;

this is also well supported by our simulations investigating the onset of lithiation at Si surfaces and Li/Si interfaces (see Supporting information, Fig. S6) as well as the previous work by Johari et al.²⁵ More fundamental explanation regarding the lithiation mechanism and kinetics will be discussed along with the results from our atomistic simulations.

By precisely tracking the reaction front movement (Fig. 1 and Movie 1), we estimated the lithiation propagation speed to be around 1082 nm/s, which is at least two orders of magnitude higher than what was reported for electrochemically lithiated SiNWs, and even five times faster than the so-called ultra-fast lithiation speed (the record-high lithiation speed of carbon coating enhanced SiNWs).²² Furthermore, our in-situ SEM study also provides insight into the kinetics of SiNW lithiation without the influences from the applied electrical field and complex reactions at the solid-electrolyte-interface (SEI). In conventional electrochemical lithiation tests, four kinetic processes are commonly considered to have effects on the rate of lithiation: (i) Li ion diffusion in the electrolyte, (ii) the redox reaction at the electrolyte/Si interface, (iii) the formation of lithiated Si (α -Li_xSi) at the interface between α -Li_xSi and c-Si, and (iv) Diffusion of the neutralized Li atoms in α -Li_xSi. Upon lithiation, Li cations (Li⁺) at the electrolyte/Si interface must combine with electrons (redox reaction) before the neutralized Li atoms can start diffusing into the Si anode. However, via the lithiation technique employed in this study, we are able to rule out the first two factors while providing a perfect controlled environment to examine the later two factors as follows.

If the α -Li_xSi alloy formation were the dominant rate-limiting factor for the lithiation speed, the corresponding length of the reaction front propagation (h) would be linearly proportional to the time (t). Otherwise, if the propagation of the effective reaction front were controlled by Li atom diffusion, the relation between h and t would followed the one-dimensional Random Walk diffusion model; $h^2 = nDt$, where n is a numerical constant depending on dimensionality and D is the diffusivity (in the reaction front advancing direction). According to the experimental results shown in Fig. 2, h^2 is linearly proportional to t (that is $h^2/t = 1.03$),

which confirms Li diffusion to be the dominant rate-limiting factor. Given one-dimensional diffusion, the Li diffusivity (D_{Li}) can be estimated around $2.58 \times 10^{-9} \text{ cm}^2/\text{s}$ based on $D = h^2/(4t)$.

Computation modelling of chemical lithiation

Still, the theoretical understanding of this diffusion-controlled chemical lithiation is very limited. Fig. 3(a) shows a schematic illustration of the potential- and electrolyte-free lithiation process considered in the present work based on the following rationales. Firstly, for a SiNW, the lithiation process is found to proceed faster along the outer surfaces than near the center.^{17, 26-28} Secondly, according to previous experimental and theoretical studies,^{21, 29} the lithiation process is much faster in the $\langle 110 \rangle$ direction, as compared to the $\langle 111 \rangle$ direction. Therefore, we can expect the lithiation of $[111]$ SiNWs to initiate preferentially at the $\{110\}$ facets. Moreover, with increasing Li contents, D_{Li} in Si tends to increase by orders of magnitude (Fig. 3b);^{28, 30, 31} this suggests that room-temperature lithiation is kinetically feasible that converts the outer surface of the c -SiNW into a - Li_xSi with x close to 4 as is in line with previously theoretical and experimental results.^{32, 33}

Given the facile Li diffusion in a highly lithiated a - Li_xSi phase, the migration of the a - $\text{Li}_x\text{Si}/\text{Si}(110)$ phase boundary near the effective reaction front, which is described in the enlarged figure in Fig. 3a, may likely be a main rate-limiting step of the entire lithiation speed. To capture the structural evolution concurrent with Li diffusion at the given phase boundary, a model cell consisting of a - Li_xSi (with x close to 4) interfaced with Si (110) facet was constructed and annealed via ab initio molecular dynamics (AIMD) simulations at 1000 K. Starting with the initial configuration ($t = 0 \text{ ps}$), the supercell after different MD time steps ($t = 4, 8$ and 16 ps) representing different stages of lithiation are shown in Fig. 4. Driven by the concentration gradient, Li atoms from the a - Li_4Si phase are diffusing across the sharp amorphous-crystalline-interface (ACI) into the c -Si matrix. The weakened c -Si lattice

(Si_A–Si_B and Si_C–Si_B bonds) eventually break off as dumbbells (Si_D–Si_B) and dissolve into the *a*-Li₄Si phase while the lithiation front advances into the pristine *c*-Si region. In a ‘layer-by-layer’ fashion, the lithiation process proceeds as the lithiation front advances approximately 4 Å in 16 ps.

Due to the difference in temperature, we cannot directly compare the calculated lithiation propagation speed (around 0.25 Å/ps at 1000 K) to the experimentally observed value (around 1 μm/s at 298 K). However, based on the one-dimensional Random Walk diffusion model ($l^2 = 2Dt$, where l is the length of the lithiation front propagation, D is the diffusivity and t is time), we could relate the lithiation propagation speed to a D_{Li} value (i.e., the simulated lithiation propagation speed of 0.25 Å/ps renders a D_{Li} value on the order of 10^{-5} cm²/s and $E_a \approx 0.3$ eV at 1000 K). Next, considering the temperature-dependent Arrhenius diffusion equation $D = D_0 \exp(-E_a/kT)$ and assuming the prefactor $D_0 \approx 10^{-3}$ cm²/s,^{28, 30, 34} we could approximate the D_{Li} value to be on the order of 10^{-9} cm²/s at room temperature (298 K), which is excellent agreement with the value estimated based on the in-situ h measurement; $D_{\text{Li}} = h^2/(4t) = 2.58 \times 10^{-9}$ cm²/s. In comparison to the wide range of experimentally measured D_{Li} values in the literature (from 10^{-14} to 10^{-8} cm²/s), our value is within the range but on the higher side, which coincides with the unprecedentedly fast lithiation process. The excellent fit between theoretical and experimental results clearly demonstrated that i) driven by the concentration difference, lithiation of a SiNW can rapidly occur in the absence of an external electric field; ii) the lithiation rate of a [111] SiNW may predominantly be controlled by the propagation of the *a*-Li_xSi/Si(110) interface as Li atoms continuously diffuse into the *c*-Si matrix leading to the advancing reaction front.

Conclusions

In conclusion, we employed a combined effort of in-situ SEM experiments and DFT calculations to investigate the concentration-gradient-driven lithiation process in individual Si nanowires (SiNWs). Through this new potential- and electrolyte-free lithiation method, we

were able to examine the genuine features of Li transport in a lithiated SiNW for the first time. The key findings of this can be summarized as follows: First, upon direct contact with Li metal, the concentration gradient is sufficient to drive the lithiation of SiNW without an applied external electrical field, which is well explained by our theoretical prediction. Similar to the electrochemically lithiated SiNWs, the chemically lithiated SiNW was also found to swell uniformly in the radial direction without noticeable elongation or bending; the total volume expansion is estimated around 330 %. Second, in-situ SEM characterization allowed us to precisely track the reaction front movement, providing significant insight into the lithiation kinetics of single crystalline SiNW. The speed of lithiation front is 1082 nm/s corresponding to the fastest lithiation speed ever recorded. We found that the square of the propagation length (h^2) is linearly proportional to the lithiation time (t), suggesting the speed of Si lithiation is controlled by how fast Li atoms diffuse across the phase boundary into the pristine *c*-Si; the Li diffusivity is estimated around $D_{\text{Li}} = 2.58 \times 10^{-9} \text{ cm}^2/\text{s}$. Finally, the observed lithiation mechanism is then cross-examined by DFT investigation, where the rate-limiting step is modeled by the propagation of the $\alpha\text{-Li}_x\text{Si}/\text{Si}(110)$ phase boundary. The predicted room-temperature D_{Li} ($\approx 10^{-9} \text{ cm}^2/\text{s}$) from our AIMD simulations is in excellent agreement with the experimentally estimated value. Our study clearly highlights that ultrafast SiNW lithiation can be solely driven by the concentration gradient in the absence of external electric field, which implies that the fast lithiation speed is primarily controlled by Li diffusion across the lithiated and pristine Si phase boundary. The fundamental findings from the combined experimental and theoretical study may extend the understanding of the lithiation kinetics in SiNWs and thereby improve the design of Si-based anodes for advanced high power LIBs.

Acknowledgements

This work was supported by KIST R&D program of 2Z04520, NST program (Grant number: Yunhap-13-1-KIST) (ISC) and the Robert A. Welch Foundation (Grant number: F-1535) (GSH). We would also like to thank the Texas Advanced Computing Center for use of their computing resources.

References

1. C. K. Chan, H. Peng, G. Liu, K. Mcilwrath, X. F. Zhang, R. A. Huggins, Y. Cui, *Nat. Nanotechnol.*, 2007, **3**, 31-35.
2. B. A. Boukamp, G. C. Lesh, R. A. Huggins, *J. Electrochem. Soc.*, 1981, **128**, 725-729.
3. M. N. Obrovac, L. Christensen, *Electrochem. Solid-State Lett.*, 2004, **5**, A93-A96.
4. T. D. Hatchard, J. R. Dahn, *J. Electrochem. Soc.*, 2004, **151**, A838-A842.
5. L. Baggetto, R. A. H. Niessen, F. Roozeboom, P. H. L. Notten, *Adv. Funct. Mater.*, 2008, **18**, 1057-1066.
6. M. Green, E. Fielder, B. Scrosati, M. Wachtler, J. S. Moreno, *Electrochem. Solid-State Lett.*, 2003, **6**, A75-A79.
7. J. Yang, M. Winter, J. O. Besenhard, *Solid State Ionics*, 1996, **90**, 281-287.
8. U. Kasavajjula, C. Wang, A. J. Appleby, *J. Power Sources*, 2007, **163**, 1003-1039.
9. J. P. Maranchi, A. F. Hepp, A. G. Evans, N. T. Nuhfer, P. N. Kumta, *J. Electrochem. Soc.*, 2006, **153**, A1246-A1253.
10. T. Takamura, S. Ohara, M. Uehara, J. Suzuki, K. Sekine, *J. Power Sources*, 2004, **129**, 96-100.
11. X. Xiao, P. Liu, M. W. Verbrugge, H. Haftbaradaran, H. Gao, *J. Power Sources*, 2011, **196**, 1409-1416.
12. I. Ryu, J. W. Choi, Y. Cui, W. D. Nix, *J. Mech. Phys. Solids*, 2011, **59**, 1717-1730.
13. X. H. Liu, L. Zhong, S. Huang, S. X. Mao, T. Zhu, J. Y. Huang, *ACS Nano*, 2012, **6**, 1522-1531.

14. B. Gao, S. Sinha, L. Fleming, O. Zhou, *Adv. Mater.*, 2001, **31**, 816-819.
15. J. L. Goldman, B. R. Long, A. A. Gewirth, R. G. Nuzzo, *Adv. Funct. Mater.*, 2011, **21**, 2412-2422.
16. S. W. Lee, M. T. McDowell, J. W. Choi, Y. Cui, *Nano lett.*, 2011, **11**, 3034-3039.
17. Q. Zhang, W. Zhang, W. Wan, Y. Cui, E. Wang, *Nano lett.*, 2010, **10**, 3243-3249.
18. H. Wu, G. Yu, L. Pan, N. Liu, M. T. McDowell, Z. Bao, Y. Cui, *Nat. Commun.*, 2012, **4**, 1943-1948.
19. X. H. Liu, J. W. Wang, S. Huang, F. Fan, X. Huang, Y. Liu, S. Krylyuk, J. Yoo, S. A. Dayeh, A. V. Davydov, S. X. Mao, S. T. Picraux, S. Zhang, J. Li, T. Zhu, J. Y. Huang, *Nat. Nanotechnol.*, 2012, **7**, 749-756.
20. M. T. McDowell, S. W. Lee, C. Wang, Y. Cui, *Nano Energy*, 2012, **1**, 401-410.
21. X. H. Liu, Y. Liu, A. Kushima, S. Zhang, T. Zhu, J. Li, J. Y. Huang, *Adv. Energy Mater.* 2012, **2**, 722-741.
22. X. H. Liu, L. Q. Zhang, L. Zhong, Y. Liu, J. W. Wang, J. -H. Cho, S. A. Dayeh, S. T. Picraux, J. P. Sullivan, S. X. Mao, Z. Z. Ye, J. Y. Huang, *Nano lett.*, 2011, **11**, 2251-2258.
23. N. Balke, S. Jesse, Y. Kim, L. Adamczyk, A. Tselev, I. N. Ivanov, N. J. Dudney, S.V. Kalinin, *Nano Lett.*, 2010, **10**, 3420-3425.
24. E. M. Pell, *Phys. Rev.*, 1960, **119**, 1014-1021.
25. P. Johari, Y. Qi, V. B. Shenoy, *Nano Lett.*, 2011, **11**, 5494-5500.
26. T. -L. Chan, J. R. Chelikowsky, *Nano Lett.*, 2010, **10**, 821-825.
27. X. H. Liu, H. Zheng, L. Zhong, S. Huang, K. Karki, L. Q. Zhang, Y. Liu, A. Kushima, W. T. Liang, J. W. Wang, J. H. Cho, E. Epstein, S. A. Dayeh, S. T. Picraux, T. Zhu, J. Li, J. P. Jullivan, J. Cumings, C. Wang, S. X. Mao, Z. Z. Ye, S. Zhang, J. Y. Huang, *Nano Lett.*, 2011, **11**, 3312-3318.
28. C. -Y. Chou, G. S. Hwang. *Surf. Sci.*, 2013, **612**, 16-23.

29. M. K. Y. Chan, C. Wolverton, J. P. Greeley, *J. Am. Chem. Soc.* 2012, **134**, 14362-14374.
30. H. Kim, K. E. Kweon, C. -Y. Chou, J. G. Ekerdt, G. S. Hwang, *J. Phys. Chem. C*, 2010, **114**, 17942-17946.
31. Z. Cui, F. Gao, Z. Cui, J. Qu, *J. Power Sources*, 2012, **207**, 150-159.
32. H. Kim, C. -Y. Chou, J. G. Ekerdt, G. S. Hwang, *J. Phys. Chem. C*, 2011, **115**, 2514-2521.
33. P. Limthongkul, Y. -I. Jang, N. J. Dudney, Y. -M. Chiang, *Acta Mater.*, 2003, **51**, 1103-1113.
34. X. R. Wang, X. Xiao, Z. Zhang, *Surf. Sci.*, 2002, **512**, 361-366.
35. G. A. Tritsarlis, K. Zhao, O. U. Okeke, E. Kaxiras, *J. Phys. Chem. C*, 2012, **116**, 22212-22216.

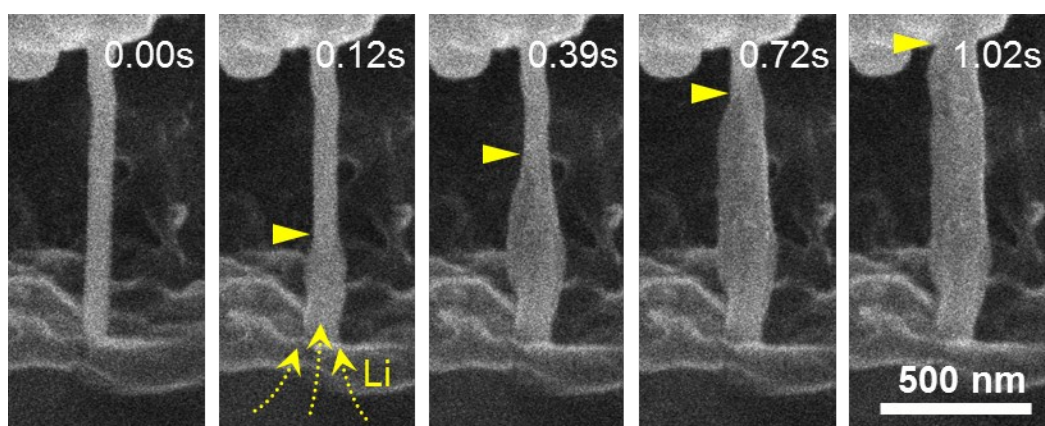


Fig. 1 Ultrafast chemical lithiation of a Si NW. Microstructural evolution of an intrinsic Si [111] nanowire in direct contact with Li metal was monitored. Volume expansion occurred instantaneously as the effective reaction front (marked by the yellow triangle) propagated from the nanowire tip towards the other end.

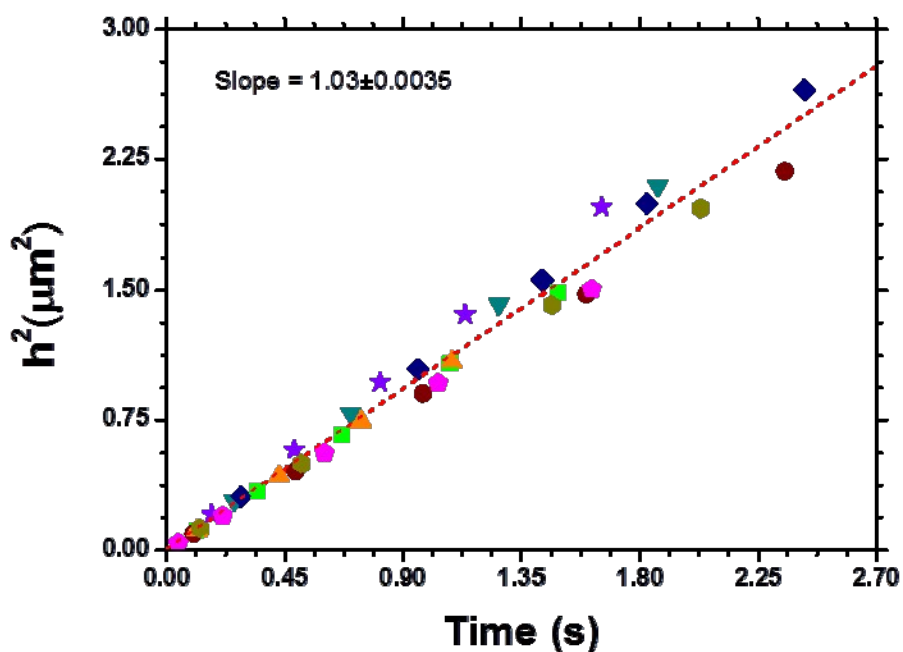


Fig. 2 The experimental plot of the length of the effective reaction front propagation (h) vs. the lithiation time (t). h^2 is linearly proportional to t ($h^2/t = 1.03$), which strongly suggests Li diffusion to be the dominant rate-limiting factor. Plots were from the nine measurements

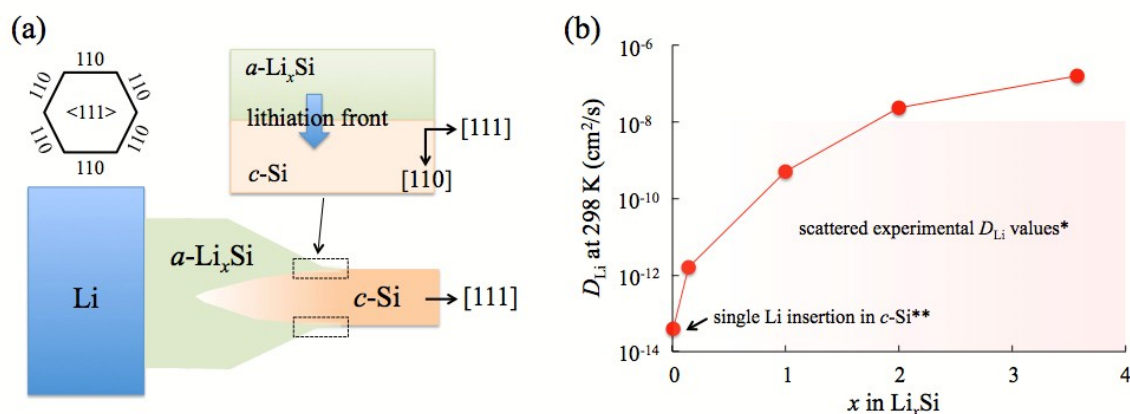


Fig. 3 (a) Schematic illustration of the model of the chemical lithiation process of a [111] SiNW. The enlarged figure for the black dotted box illustrates a- $\text{Li}_x\text{Si}/\text{Si}(110)$ phase boundary near the effective reaction front. The phase boundary (the lithiation front) moves from the outers surface into the center, which is rationalized as the rate limiting step of the propagation of the effective reaction front. (b) Variations in diffusivity (D_{Li}) of Li atoms in a- Li_xSi alloys of selected Li contents ($x = 0.02, 0.14, 1, 2$ and 3.57) at 298 K; an example of how D_{Li} can be predicted based on AIMD simulations is shown in Figure S7. For comparison, the scattered experimental D_{Li} values and D_{Li} calculated for a single Li in c-Si are indicated by *²⁸ and **³⁰, respectively.

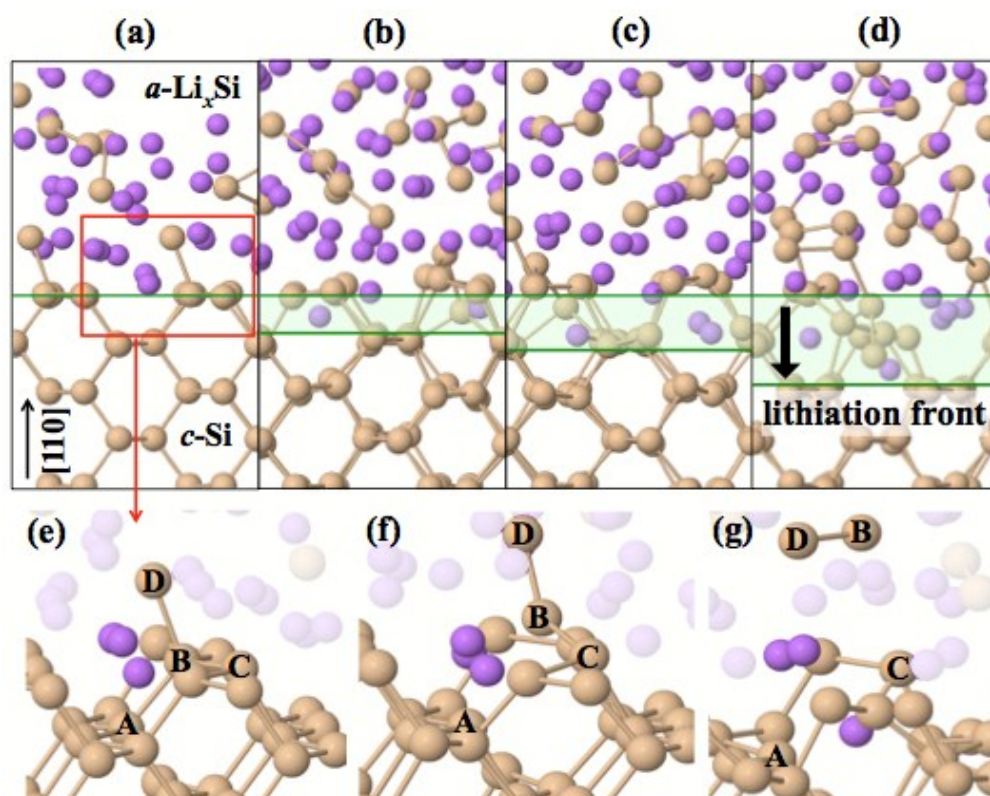


Fig. 4 AIMD simulation to capture the structure evolution of the a- $\text{Li}_x\text{Si}/\text{Si}(110)$ phase boundary at various stages of lithiation; structures shown in (a) to (d) correspond to the starting $t = 0$ and after 4, 8 and 16 ps of annealing at 1000 K. The breakoff of Si-Si dumbbells is captured in configurations shown in (e) to (g).

Graphical Abstract

